Optogentics and Optrode Technology to Brain Function Manupulation

Mohammad Ismail Zibaii[1], Leila Dargahi[2], Abdolaziz Ronaghi[2], Farshad Abedzadeh[1], Sareh Pandamoz[2], Saeid Salehi[2], Zahra Fattahi[3], Abbas Haghparast[3] and Hamid Latifi[1]
[1]*Laser and Plasma Research Institute, Shahid Beheshti University, Tehran, Iran*
[2]*NeuroBiology Research Center, Shahid Beheshti University of Medical Sciences, Tehran, Iran*
[3]*Neuroscience Research Center, Shahid Beheshti University of Medical Sciences, Tehran, Iran*
{m_zibaye, latifi}@sbu.ac.ir, haghparast@yahoo.com, l.dargahi@sbmu.ac.ir

Keywords: Optogenetics, Optrode, Fiber Optic, Channelrhodopsin, Optical Stimulation, Neural Recording.

Abstract: Optogenetics comprises a growing family of related techniques for the optical interrogation and control of excitable cells. Combining genetic targeting with light delivery systems makes it possible to drive or silence subpopulations of neurons and the related behaviours, with a high spatiotemporal precision. Since optical manipulation is fast, selective, and minimally invasive, it provides distinct advantages over traditional electrical means or pharmacological approaches for cell perturbation. Here we showed in anesthetized rat that optogenetic stimulation of nucleus accumbens (**NAc**) neurons increased neural activation. We labelled a population of neurons activated with channelrhodopsin-2 (ChR2) and later optically stimulated these neurons by using an optrode and recorded spontaneous action potentials from the one neuron.

1 INTRODUCTION

One of the main goals of systems neuroscience is to understand the architecture and function of neural circuits. These circuits consist of a complex network of varying neural subtypes. The development of technologies to regulate the activity of specific types of cells is key to understanding how they contribute to local network activity and overall brain function *in vivo*. Classical neuronal manipulation techniques such as electrical (Hales, 2010), pharmacological (Gorostiza, 2008) and genetic ultrasound (Tufail, 2010) either simultaneously affect surrounding cells and processes in addition to the target population or have slow kinetics and poor reversibility.

To overcome these spatial and temporal limitations, optogenetics have been developed based on optical control of genetically targeted biological systems (Deisseroth, 2006). Optogenetic techniques provide a means of activating or inhibiting distinct populations of neurons via light-sensitive microbial membrane proteins at high temporal and spatial resolution. As most neurons in the brain are not naturally light-sensitive, selective expression of opsin genes in targeted neural populations makes it possible to specifically control the activity in these populations, and the resulting fast on–off kinetics make it possible to evoke or inhibit neural activity within milliseconds, on a timescale relevant to the physiological brain functions (Boyden, 2005) . A remarkable feature of the optogenetic approach is the ability to target probes to genetically defined cell types and subcellular compartments, which allows the probes to be used for investigating multiple levels of nervous system function. Fig. 1 illustrates the various levels at which optogenetic strategies can be used to manipulate function within mammalian neural circuits.

The most common light-sensitive protein in use today is channelrhodopsin-2 (ChR2), an algal protein from Chlamydomonas reinhardtii. It is a light-activated cation channel capable of transducing millisecond long flashes of blue light into defined spike trains as fast as 30- 50 Hz (Adamantidis , 2007; Gunaydin, 2010).

Optogenetic approaches have been successfully used in vitro to study basic synaptic properties of specific neural circuits as well as in vivo to study the role of such circuits in physiology and behaviour (Berndt, 2011; Franklin, 2015; Packer, 2015). The use of optogenetic tools to stimulate or suppress the activity of neural populations has potential applications for both experimental and therapeutic

approaches (Krook-Magnuson, 2015).

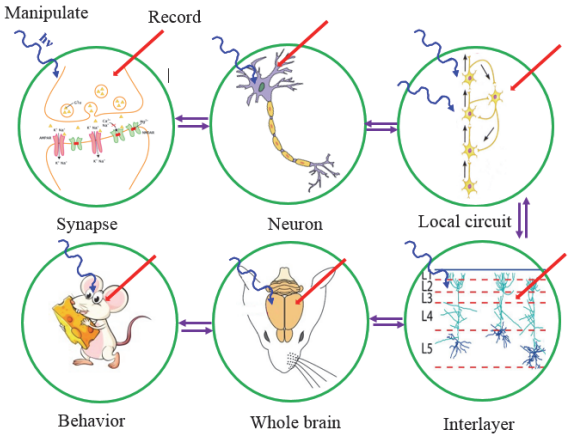

Figure 1: Optogenetics can be applied at all levels of brain function. A variety of applications use optogenetic probes to both read out and manipulate activity. Specificity can be achieved either by targeting probe expression to relevant cellular compartments or network elements or by targeting light to these elements. The ability to implement optogenetics at different levels of nervous system function provides a powerful way to make causal links between these levels.

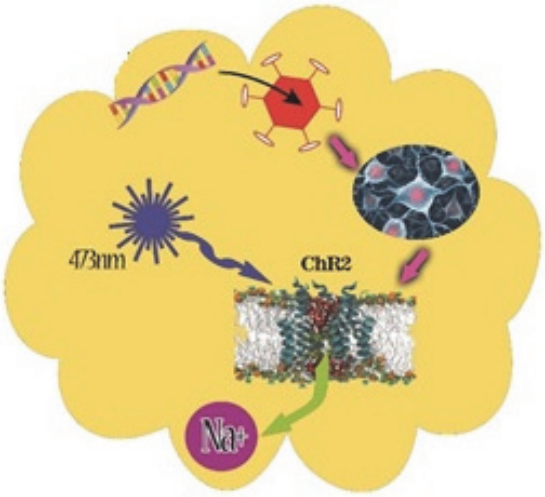

Figure 2: Making neurons react to light: For optogenetic studies, neuroscientists insert opsin genes into brain cells with the aid of engineered viruses. They can then trigger neural activity on demand with flashes of light and observe the effects on experimental animals' behavior.

In this paper we presented several aspects including challenges for light delivery in living brain tissue, the combination of light delivery with electrophysiological recordings and probe designs for optogenetics technique. Also, we applied this technique for simultaneous optical stimulation and electrical recording by using a simple optrode in the nucleus accumbens (**NAc**). In Figure 2 all of our procedure were shown which includes viral packaging, virus injection, gene expression in NAc, and light stimulation of ChR2 ion channels.

2 PHYSICS OF OPTOGENETICS

Brain tissue is not transparent to visible light and one of the main challenges for the use of optogenetics in vivo is the limited light penetration and confinement in deeper structures. Once the fibers is placed close to the target area, light is emitted with a known power density. However, as the light exits the fiber, it is scattered and slightly adsorbed by the tissue, so that the target area beyond the fiber will be actually illuminated with a strong intensity gradient. The properties of light transmission in brain tissue have been largely characterized, and were shown to be strongly dependent on the wavelength, with higher absorption recorded for shorter wavelengths. Indeed, due to light scattering and absorption, a usable amount of visible light cannot easily reach deep brain structures and illumination from an external source is, in practice, limited to the cortex. Light intensity attenuation and spread in brain tissue have been measured and then fit with standard equations for light propagation in scattering media to establish a model for estimating the light power density at the points further from the fiber exit.

The Beer–Lambert equation can be used to estimate light attenuation after propagation in tissue:

$$I(z) = I_0 e^{-\mu_z(\lambda) z} \quad (1)$$

In Eq. (1), I (z) stands for the light intensity after a travelled distance of z, I_0 is the initial intensity, and μ_t is the extinction coefficient. This coefficient can be calculated from the absorption and scattering coefficient in biological tissue, $\mu_a(\lambda)$ and $\mu'_s(\lambda)$, respectively:

$$\mu(\lambda) = \mu_a(\lambda) + \mu'_s(\lambda) \quad (2)$$

Both $\mu_a(\lambda)$ and $\mu'_s(\lambda)$ depend on the wavelength, λ. Note that light scattering in tissue is anisotropic, meaning that light will scatter with preferential angles. The value $\mu'_s(\lambda)$ thus incorporates an anisotropic factor, g:

$$\mu'_s = \mu_s(1-g) \quad (3)$$

Optical fibers thus offer a convenient alternative to reach deeper structures. Two main aspects are important when choosing the right fiber: the optical fiber core size, which should be in the same order of magnitude than the targeted area, and the optical fiber

numerical aperture (NA). The later influences the transversal spread of the illumination volume and is defined as

$$NA = \sqrt{n_1^2 - n_2^2} \quad (4)$$

where n_1 and n_2 are the refractive indices of the fiber core and cladding, respectively.

Knowing these values and those of tissue optical properties (extinction coefficients and refractive index), one can easily estimate the effective excitation volume at the fiber tip.

The complete relationship of light intensity to tissue penetration distance was estimated by taking the product of the measured transmission fraction (remaining light not scattered or absorbed) and the calculated fractional decrease in intensity due to the conical geometry of emitted light at a given distance in the absence of tissue scattering and absorption. The half-angle of divergence θ_{div} for a multimode optical fiber is

$$\theta_{div} = \sin^{-1}\left(\frac{NA_{fib}}{n_{tis}}\right) \quad (5)$$

where n_{tis} is the index of refraction of gray matter and NA_{fib} is the numerical aperture of the optical fiber (Ray, 1991 and Vo-Dinh, 2003).

Assuming conservation of energy, the geometric decrease in intensity with distance from the fiber end z was calculated (Aravanis, 2007):

$$\frac{I(z)}{I(z=0)} = \frac{\rho^2}{(z+\rho)^2} \quad (6)$$

Where

$$\rho = r\sqrt{\left(\frac{n}{NA}\right)^2 - 1} \quad (7)$$

where and r is the radius of the optical fiber. The complete expression for intensity taking into account both the scattering and geometric losses is

$$\frac{I(z)}{I(z=0)} = \frac{\rho^2}{(\mu_s' + 1)(z+\rho)^2} \quad (8)$$

For neuron activation, the outer limit of this volume that can be defined has the minimal intensity value for action potential generation. This value will differ from one protein to another and from one subject to another since the membrane expression level of the protein may vary. The volume of activation can always be enlarged by increasing light intensity at the fiber tip, but this intensity must be kept below tissue damage threshold. This threshold will be different for the different protocols used and is dependent on the stimulation duration and repetition rate, but in most cases an intensity at the fiber tip around 300 mW⁄mm^2 was reported to be safe. However, for sustained stimulation, damages were reported at levels above 100 mW⁄mm^2. Using this input intensity at the tip of an optical fiber of 200 µm core diameter with an NA of 0.2, the limit for ChR2 activation (1 mW⁄mm^2) is reached at a distance of ≈2 mm. The dashed line represents the1 mW⁄mm^2 activation threshold.

ChR2 is both light and voltage-sensitive. Figure 3 shows the schematic of ChR2 mechanism. The conducting pore of the channel associates (via a covalent bond) to retinal, which serves as the chromophore (the light-sensing element). Interaction of all-transretinal with a photon of the proper wavelength (470 nm) leads to instantaneous isomerization to 13-cis-retinal. This transition triggers the opening of the ion channel allowing cation movements down their electrochemical gradient, with preferential selectivity to H^+ (Nagel, 2003; Lin, 2009). ChR2 at negative membrane potentials provides exclusively inward current with a reversal potential near 0 mV. The single channel conductance for the wild type ChR2 is small compared to classical excitatory ion channels (e.g. sodium channels) with reported values ranging from 40–90 Fs (Zimmermann, 2008 and Nagel, 2003) to 0.25–2.42 ps (Lin, 2009). Genetically engineered mutants of ChR2, e.g. H134R yields larger photocurrents relative to wild-type ChR2, but with slower K_{off} kinetics.

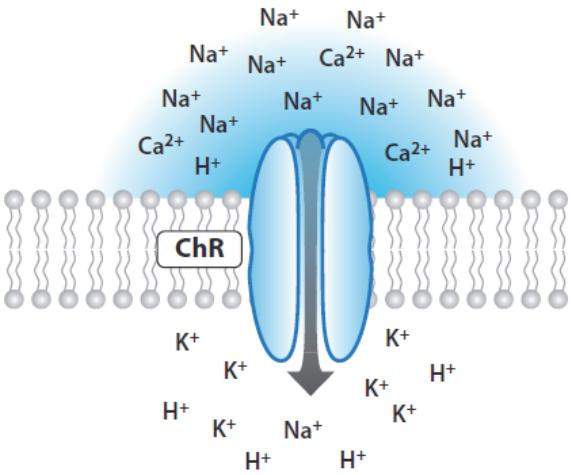

Figure 3: Channelrhodopsins conduct cations and depolarize neurons upon illumination.

For a genetically based photostimulation method, the magnitude of the response depends as well on the total number of ChR2 proteins that are illuminated, which is a function of the expression level. Although single-channel studies have not been performed, ChR2 has been estimated to possess a single-channel

conductance as low as 50 femtosiemens (Nagel, 2003). This would imply that between 100,000 and 1,000,000 ChR2 molecules would have to be generated and localized to the neuronal membrane to achieve the observed currents in the range of 1 nA which is starting from a resting potential of –70 mV and neglecting space-clamp issues and changes in driving force due to ion entry (Zhang, 2006).

3 MATERIAL AND METHODS

3.1 Light Sources

The choice of the light source is dictated by the experimental needs in terms of light power and frequency of light pulses. Either laser (diode or diode-pumped solid state, DPSS) or light-emitting diodes (LED) have been conveniently employed in optogenetics experiments (Kale, 2015). Figure 4 show LEDs and a DPSS laser. Blue wavelengths are needed for excitatory ChR while yellow wavelengths are required for inhibitory Halorhodopsins. Lasers have the advantage of having a very narrow spectral linewidth (less than 1 nm), which is particularly useful in the case of experiments with multiple opsins with different peak activation wavelengths. Moreover, laser beams have very low divergence, allowing for an easy and straightforward light manipulation by means of mirrors and lenses and therefore a highly-efficient coupling into optical fibers. Disadvantages of lasers are high cost, especially for yellow lasers, long warming times, and stability. Moreover, problems can be encountered when high speed modulation is required, especially for yellow DPSS lasers (Aravanis, 2007).

LEDs are instead low cost, do not need complex control electronics and can be easily modulated at the millisecond scale. Main disadvantages of LEDs are a relatively wide spectral linewidth (a few tens of nm) and a pronounced beam divergence and broad emission pattern, which hinders a good LED-to-fiber coupling as needed to deliver high light powers. LEDs integrated on the device to be implanted have also been employed (Kim, 2010). The main advantage of using on-implant LEDs is that LEDs are driven by an electrical signal, which allows using only electrical connecting cables when combined with recording electrodes. However, due to the poor coupling with optical fibers, local LEDs have been mostly employed as local light source for surface illumination or implanted in the tissue as miniaturized micro-LEDs (Grossman, 2010). Using local LEDs enable the realization of wireless systems where the LED driving electrical power is transmitted and/or modulated with a radio link. As a main drawback, full operation of these systems is limited by the generated heat.

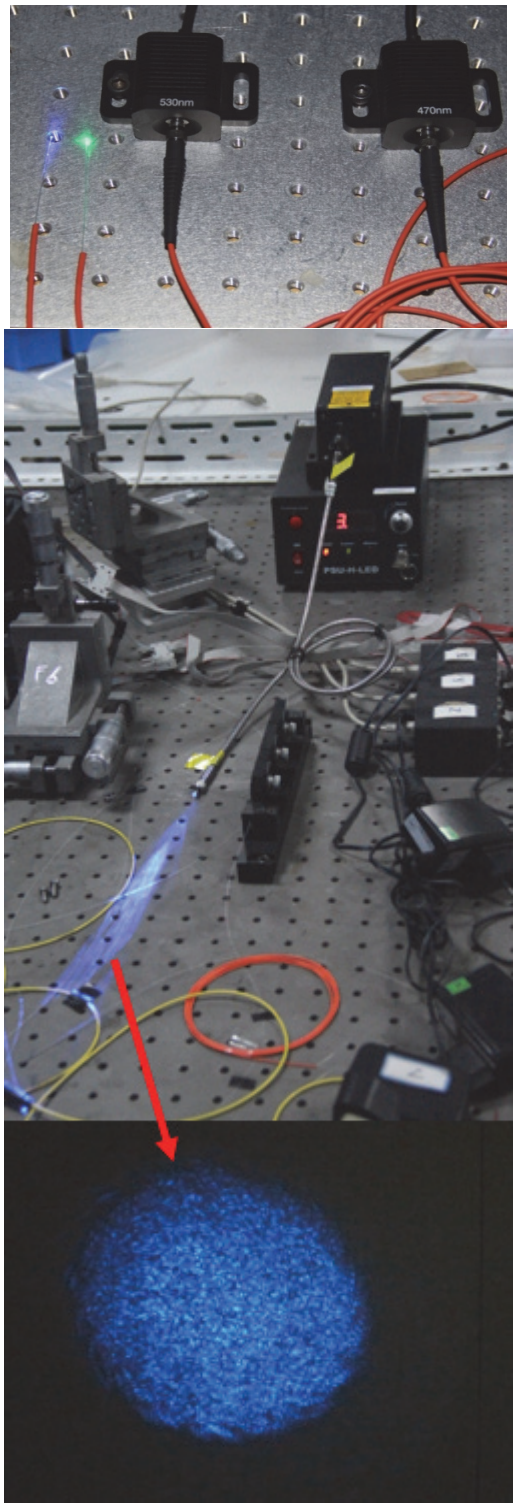

Figure 4: LED and DPSS laser as light source in optognetic technique.

3.2 Fiber Optic Approaches for Light Delivery in Vivo

Different experimental paradigms adopted for optogenetic actuation of neurons correspond to specific spatio-temporal light delivery approaches. For example, short light pulses and small duty cycles are used in the case of bistable optogenetic control (Yizhar, 2011 and Sileo, 2015), whereas continuous light delivery is needed for inhibition of neurons (Yizhar, 2011). As well, different light delivery methods need to be employed for different target regions. Microscope objective are mostly used for optogenetic control of cortical layers (Bovetti, 2015 and Losonczy, 2010), while fiber optics-based implants are the most widely spread technology for accessing deep brain regions.

Using a standard fiber optic is by large the most employed approach for optogenetic investigation of deep brain targets. However, the implantation of a fiber optic invariably causes a certain degree of mechanical damage to the brain tissue and often localized bleeding, especially when large core fibers are used for high light power delivery needs. For applications requiring multipoint illumination (Warden, 2014 and Sileo, 2015), such as in bilateral stimulation, illumination of large volumes, or illumination of multiple sites with specific spatial patterns, using multiple standard optical fibers leads to major invasiveness issues.

Technological efforts have been made to realize miniaturized, micro-fabricated waveguides (Abaya, 2012 and Zorzos, 2012), which were also integrated with recording electrodes or with LEDs (Stark, 2013).

The first optical neural interface successfully used for optogenetic neural interfacing in anesthetized (Aravanis, 2007) and freely behaving (Adamantidis, 2007) rodents. In this approach, a cannula is implanted in the skull above the target region and used as the guide for both the needle used for viral injection for opsins genetic encoding and the fiber optic. This system assures the co-registration between opsin-expressing and illuminated brain volumes, allows targeting regions with different depths and, remarkably, it permits to combine optogenetic and pharmacological manipulations.

A second largely employed system consists on the use of a permanently implanted fiber, connectorized at one end with a ceramic ferrule which remains just outside the skull (Sparta, 2012 and, Zhang, 2010). Figure 5 shows a fiber optic cannula. Connection with the light source through a patch cord is made only at the time of the experiment with the mating sleeve system.

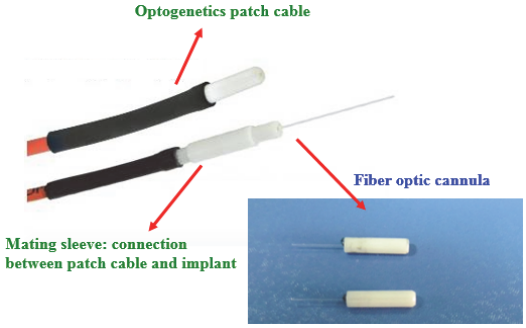

Figure 5: Fiber optic patch cable connected to a fiber optic cannula.

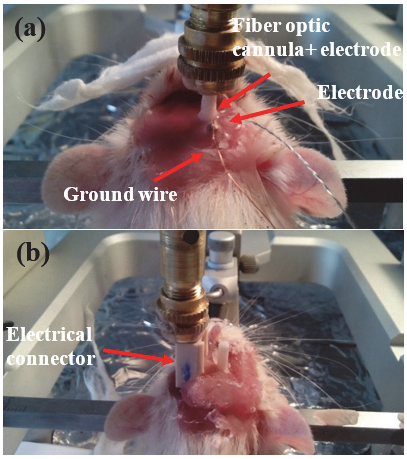

Figure 6: Impelantation of (a) fiber optic cannula and (b) electrode for freely moving.

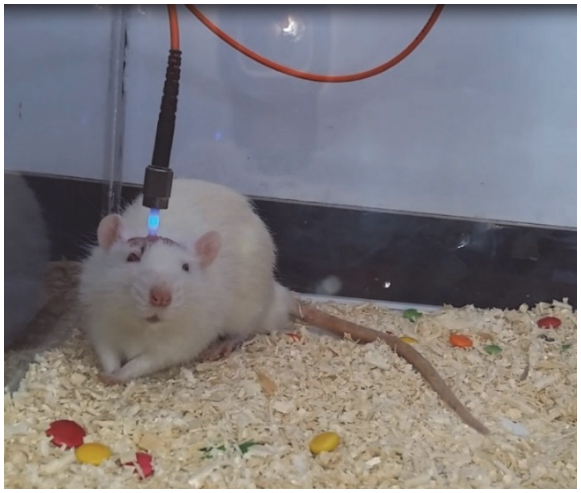

Figure 7: Inmplanted fiber optic cannula in freely moving rat.

Figure 6 shows a fiber optic cannula which is stereotactically implanted in the target area. As is

shown in figure 7 in experiments with freely moving animals the fiber is coupled with a light source.

This system has the advantage of reducing tissue damage from repeated fiber insertions, as well as the risk of infection. Although the co-registration capability of the cannula system is lost, the ferrule implant system is ideal for high-throughput behavioral experiments with chronic implants. Figure 8 shows a fiber optic cannula after removing of implantation.

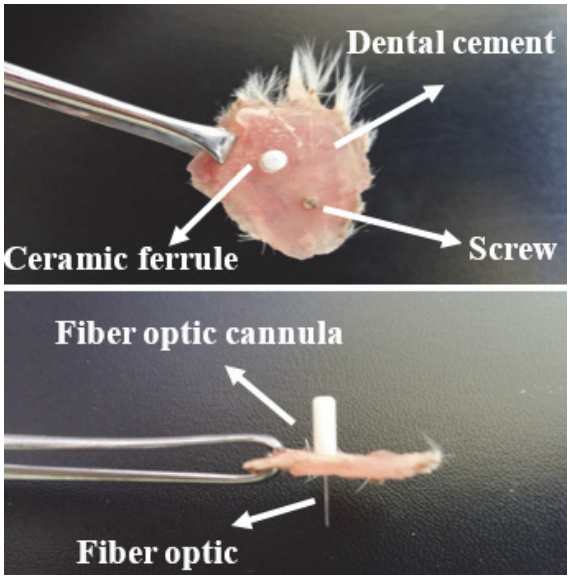

Figure 8: Fiber optic cannula after removing of implantation.

Also, in optogenetics experiments with live animals for the free movement of animal and fiber optic cables with a minimum of torque while maintaining excellent light transmission can be used a fiber optic Rotary Joint (FORJ). Figure 9 shows a FORJ which fiber optic leads of these cables are permanently attached to the rotary joint for higher performance and provide a one piece, integrated fiber optic solution. For compatibility with a wide range of cannulae, light sources, and experimental setups, there are rotary joint cables using fibers with different core sizes and NAs. There are cables with different connectors or any length of fiber on each end of the joint. For best performance, the fiber core size should be 200 µm or greater.

Figure 9: A FORJ for coneting of the light source to implanted fiber optic cannula for freely moving experiments.

Two point light delivery can be simply realized with two separately implanted cannulas or ferrules, the minimum distance between the two target sites becoming the main limitation. Using more than two fibers for studying photo-activation patterns becomes prohibitive with standard approaches. Some alternative approaches have been proposed for multipoint light delivery with standard optical fibers and tapered fibers (Pisanello, 2014, Dufour, 2015).

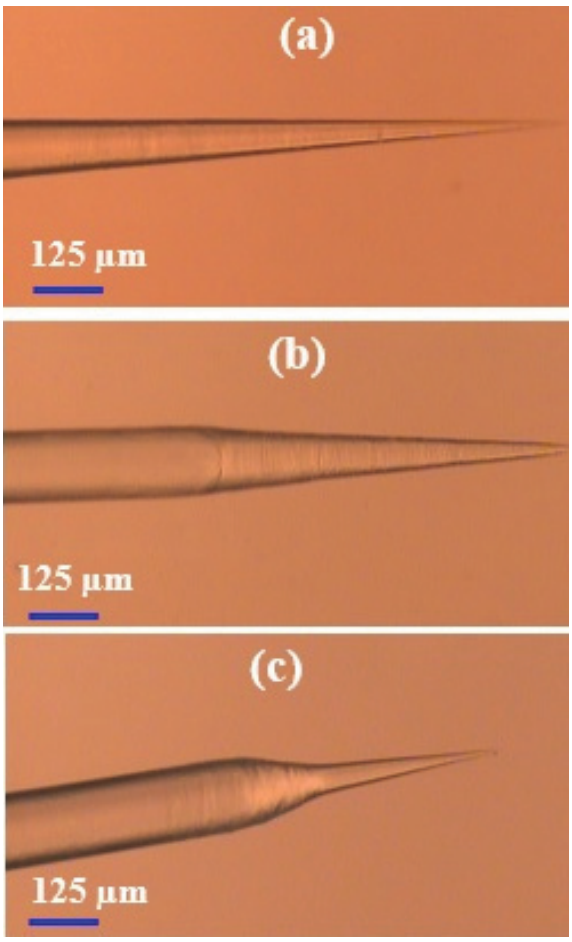

Figure 10: Tip fiber optic with different tip profiles.

Tapered fibers, i.e. fiber optics with a tip that is chemically (Andre, 2015) or thermo-mechanically etched down to sub-micrometer diameters have been used to reduce the insertion damage of fiber optics.

However, their use for optogenetic light delivery is limited by the lack of a complete optical characterization, even when peculiar light emission properties of tapered fibers can potentially explain new optogenetic manipulation capabilities, which cannot be achieved with a standard optical fiber (Royer, 2010). Figure 10 shows different tapered fiber tips which are fabricated with chemical etching method (Andre, 2015). A SEM photo of tapered fiber tip is shown in figure 11.

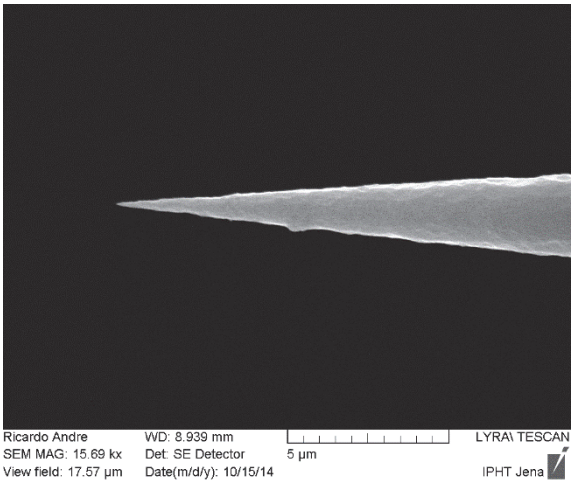

Figure 11: SEM micrographs of tapered fiber tips.

3.3 Optrode Fabrication

Compared with electrical stimulation, the optical method offers a seamless solution to the problem of cross-talk generated by simultaneous electrical stimulation and recording. To optically manipulate and electrophysiologically record neural activity for anesthetized animal, we developed a dual-function device which is named optrode. As is shown in figure 12 the optrode is made by simply gluing a step index fiber optic with core diameter 200 µm to a tungsten microelectrode for anesthetized recording. The total fiber diameter with cladding is 20 to 30 µm larger, thus resulting in an overall implant cross section of few hundreds of micrometers.

It should be noted that the optical excitation generates photoelectric artefacts that interfere with electronics (Kozai, 2015). One important characteristic of the photoelectric effect is that electrons are only dislodged by the photoelectric effect if light reaches or exceeds a threshold frequency, below which no electrons can be emitted from the electric conductor regardless of the amplitude and temporal length of exposure of light. In this study for controlling of photoelectric effect the fiber tip is placed in certain distance of the electrode.

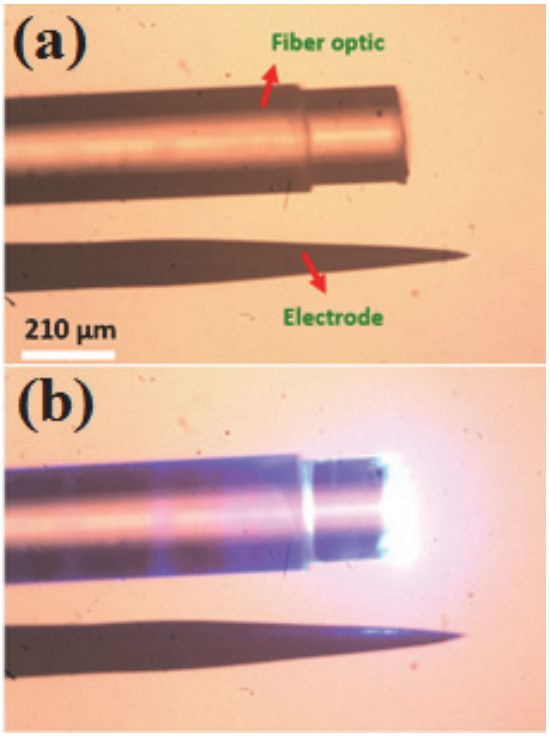

Figure 12: (a) The self-designed optrode, and (b) illumination of blue light from tip of fiber.

3.4 Stereotactic Implantation of the Guide Cannula

Male Wistar rats weighing about 280 g were anesthetized with Ketamine (80 mg/kg, i.p.) and xylazine (10 mg/kg, i.p.) with supplemental doses as required. After mounting the animal into the stereotactic frame, a first incision is made to open the skin above the skull. The skin is gently pulled to the side to reveal the cranial sutures. After quickly wiping the skull with hydrogen peroxide, the bregma and the lambda can be easily identified (marked spots). With a dental drill a small craniotomy was created at the desired location on the skull, without puncturing the dura. The dura is later removed using fine forceps to minimize damage to the cortex. A guide cannula is then implanted on the skull targeting nucleus accumbens in right brain hemisphere. Metabond and dental cement are used to secure the cannula guide to the skull. The animal is allowed to rest in a recovery cage after surgical implantation. The surgery was

conducted according to established animal care guidelines and standard protocols (Riahi, 2015).

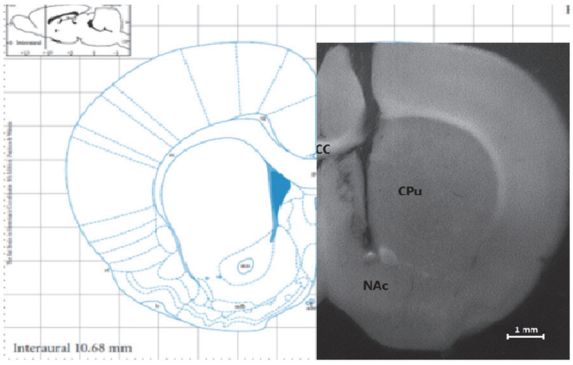

Figure 13: A coronal photomicrograph of unilateral microinjection and optic fiber sites in the nucleus accumbens of rat. aca, anterior commissure, anterior part; CC, corpus callosum; CPu, caudate putamen (striatum); NAc, nucleus accumbens.

3.5 Virus Injection

ChR2 can be stably introduced into tissues through techniques such as viral delivery, creation of transgenic lines or electroporation. Lentiviral technology provides a convenient combination of stable long-term expression and ease of electrophysiological validation of functional expression. Unlike the generation of transgenic animals, lentiviruses can be produced in days, and stable gene expression can be observed as early as 8 days after infection.

In this study we used lentiviral plasmid DNA encoding ChR2 (pLenti-CaMKIIa-hChR2(H134R)-mCherry-WPRE, Optogenetics.org), obtained from Stanford University and amplified using standard methods in molecular biology (MidiPrep, QIAGEN).Viral injection for ChR2 expression was conducted 24 h after guide cannula implantation with consequent three times by interval 72 h.

A convection driven injector with a hypodermic needle (G32 Hamilton) was slowly driven into the pre-defined NAc through the guide cannula. Prior to actual injection, we advanced the needle beyond the target depth by 100 µm and retracted it by the same distance to create a vacuous cavity. Injection was made in target place with coordination of 1.7 mm AP, +1.4 mm ML and -7.0 mm DV according to the atlas of Paxinos and Watson, 6th Ed. Viral solution was injected at a speed of 0.1 µL min^{-1} and volume of 1 µL. After injection solution the needle leaved in place for 10 additional min to allow the virus to diffuse in the target zone.

To confirm transgene expression, immunohistochemical analysis was performed on paraffin-embedded brain coronal sections using antibody against mCherry and HRP-DAB visualization system, after electrophysiological recordings.

4 EXPERIMENTAL SETUP

Three weeks after last virus injection, rats were deeply anesthetized with Urethane (1.5 g/kg, i.p., with supplemental doses as required; Sigma–Aldrich, Germany) and mounted into the stereotactic frame. To reduce the respiratory efforts and maintain an open airway during the recording, the rats were subjected to surgical tracheostomy.

To record the neural activity in NAc area under optical stimulation, a homemade single unit recording setup was used. The electrical signal was filtered (300–6,000 Hz) and amplified. The optrode was propagated via the mechanical drive to the recording site at least 30 min before the experiment to ensure stable recordings. Optical stimulation was applied through an optical fibre attached to the fibre-ferrule of the optrode. For optical stimulation of the NAc in ChR2-expressing rat, we used a blue laser diode (λ =473 nm, thorlabs) pulsed at 20 Hz, with 25 ms pulse width and a power density of 60–160 mW mm^{-2} at the tip of the fiber. Before starting any stimulation, the input–output function of the laser should be tested

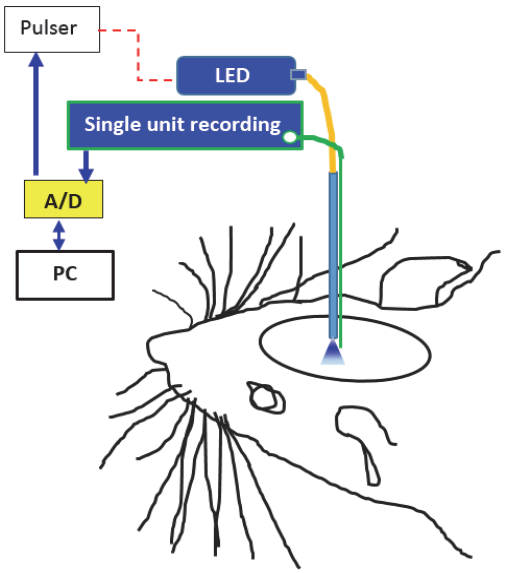

Figure 14: Schematic of experimental setup for simultaneous optical stimulation and electrical recording by using optrode, containing optrode, LED, Pulser, single unit recording system, A/D, and PC.

with the optical power meter. The light power at different distances from the fiber tip was estimated as a function of both wavelength and the power of light at the fiber tip. Only a low total output power may be needed to achieve ChR2 activation. For instance, 2 mW at the tip of a 200-μm core diameter fiber corresponds to 64 mW mm^{-2}, well above the minimal effective range for in vivo stimulation. Schematic of experimental setup is shown in figure 14.

5 EXPERIMENTAL RESULTS

Depending on targeted cell type, the maximal evoked firing frequency will vary. Spiking properties in targeted cells depend on spike and illumination history as well as on membrane expression level of ChR2 and local illumination intensity; for any given cell type and circuit, a detailed characterization should be carried out to determine the efficacy of light evoked spike trains. To track and validate activity modulation, optrode recordings can be carried out *in vivo*. Artifacts, although much smaller than for electrical stimulation, can be occasionally observed; when present, such artifacts are correlated with the onset and offset of the light pulse; amplitude depends on light power and can be reduced with proper grounding and use of electrodes with coating extending to the tip and staggered relative to the optical fiber by 300–500 μm, as is typically important in any case for proper illumination of the recorded area (Ozden, 2013).

The neuron activity in the NAc area under different optical stimulations were recorded by using optrode. A photo of experimental setup for optical stimulation of anesthetized rat is shown in figure 15. Typical raw electrophysiological recordings before and after optical stimulation were shown in figure 16. The raw data shows that with optical stimulation the firing rate of the same neuron can be increased. A typical expanded waveform of a spike generated form one of the NAc neurons in an anesthetized rat was shown in figure 17.

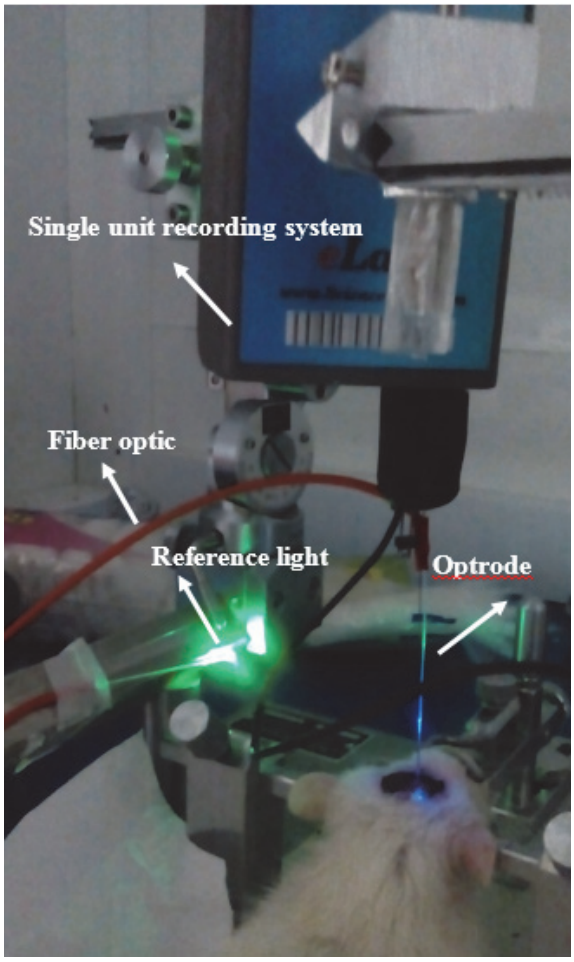

Figure 15: A photo of anesthetised rat optical stimulation and electrical signal recording by using optrode in optogenetic technique, containing fiber optic, optrode and reference light.

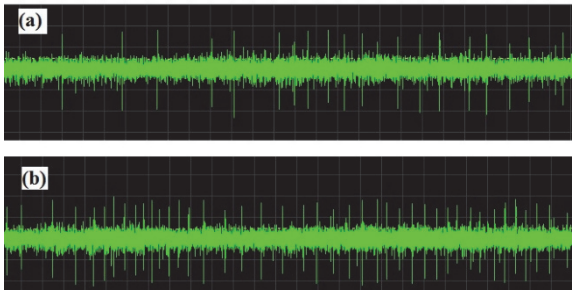

Figure 16: Raw data of the neuron activity recorded from anesthetized ChR2-expressing rat by using optrode. The trace (a) representing recording of single unit activity from the NAc of an anesthetized rat. The trace (b) representing recording of single unit activity from the same neuron after optical stimulation.

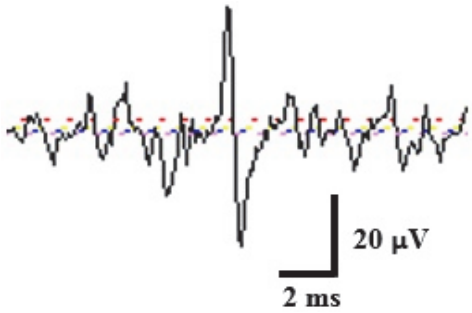

Figure 17: An expanded waveform of a spike generative form one of the NAc neurons.

The figure 18 shows the histogram of spike firing rate per bin. As shown in this figure optical stimulation caused to significant in histogram bars. The dash line indicate the duration of light illumination.

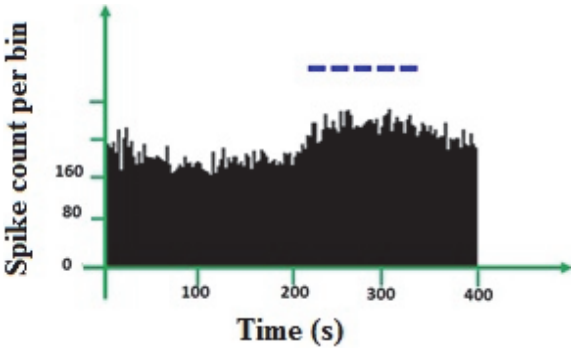

Figure 18: Histograms representing spike count per bin over the entire recording the firing frequency of one recorded neuron. Stimulation by blue light increased the firing frequency of the recorded neuron.

After the electrophysiological experiments, the rat was sacrificed to check the virus expression and fiber tip position. Figure 19 shows a representative coronal brain section immunostained against mCherry.

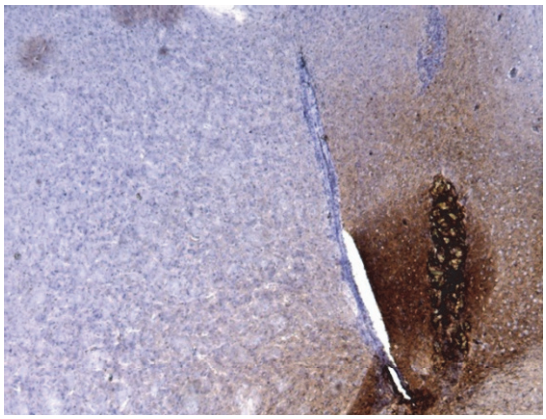

Figure 19: Coronal section of rat brain immunostained for mCherry, at 10x objective magnification.

6 CONCLUSIONS

We employed optogenetic manipulations based on viral transduction of ChR2 in the brain region of NAc and by using an optrode in the same time, signal of one neuron was recorded. The results demonstrated that optogenetic activations of the excitatory neurons expressing CaMKIIα in the NAc able to activate the neuron. Moreover, this study has provided a novel method to optically stimulation of the neuron. Also, Optrodes are important in the study of brain function, especially using the method of optogenetics. We believe the optogenetics and optrode technology will likely play a crucial role in contributing to our deep understanding of how diverse classes of neural circuit components interact to give rise to complex behaviors, pathological conditions, and therapeutic responses.

ACKNOWLEDGEMENTS

This work was supported by the Cognitive Science and Technologies Council of Iran (CSTC). We thank Prof. Fereshteh Motamedi and Prof. Abolhassan Ahmadiani for useful discussion.

REFERENCES

Abaya, T., V., Blair, F., S., Tathireddy, P., Rieth, L., Solzbacher, F., A., 2012. 3D glass optrode array for optical neural stimulation, *Biomed. Opt. Express*, vol. 3, pp. 3087–3104.

Adamantidis, A.R., Zhang, F., Aravanis, A.M., Deisseroth, K. & de Lecea, L., 2007. Neural substrates of awakening probed with optogenetic control of hypocretin neurons. *Nature* 450, 420–424.

Aravanis, A., M., Wang, L., P., Zhang, F., Meltzer, L., A., Mogri, M., Z., Schneider, M., B., Deisseroth, K., 2007. An optical neural interface: in vivo control of rodent motor cortex with integrated fiber optic and optogenetic technology, J. Neural Eng., vol. 4, pp. S143–156.

André, R., M., Becker, M., Dellith, J., Manfred Rothhardt, M., Zibaii, M., I., H. Latifi, H., Marques, M., B., Bartelt, H., Frazão, O., 2015. Bragg grating fabrication on tapered fiber tips based on focused ion beam milling. *Proc. SPIE* 9634.

Berndt, A., Schoenenberger, P., Mattis, J., Tye, K.M., Deisseroth, K., Hegemann, P., Oertner, T.G., 2011. High-efficiency channelrhodopsins for fast neuronal stimulation at low light levels. Proc Natl Acad Sci USA; 108(18):7595–7600.

Boyden, E.S., Zhang, F., Bamberg, E., Nagel, G., Deisseroth, K., 2005. Millisecond-timescale, genetically targeted optical control of neural activity. *Nat Neurosci*.; 8(9):1263–1268.

Bovetti, S., T. Fellin, T., 2015. Optical dissection of brain circuits with patterned illumination through the phase modulation of light, *Journal of Neuroscience Methods*, vol. 241, pp. 66-77.

Deisseroth, K., Feng, G.P., Majewska, A.K., Miesenbock, G., Ting, A., Schnitzer, M.J., 2006. Next-generation optical technologies for illuminating genetically

targeted brain circuits. J Neurosci.; 26(41):10380–10386.

Dufour, S., De Koninck, Y., 2015. Rewiev: Optrodes for combined optogenetics and electrophysiology in live animals, *Neurophotonics* 2(3), 031205-14.

Feldbauer, K., Zimmermann, D., Pintschovius, V., Spitz, J., Bamann, C., et al. 2009, Channelrhodopsin-2 is a leaky proton pump. Proc Natl Acad Sci USA 106: 12317–12322.

Franklin, G.F., Powell, J.D., and Emami-Naeini, A., 2015. Feedback control of dynamic systems. (New York: Prentice Hall).

N. Grossman, V. Poher, M.S. Grubb, et al.: Multi-site optical excitation using ChR2 and micro LED array, J. Neural Eng. vol. 7, pp. 16004, 2010.

Gorostiza, P., Isacoff, E.Y., 2008. Optical switches for remote and noninvasive control of cell signaling. Science.; 322(5900):395–399.

Gunaydin, L.A., Yizhar, O., Berndt, A., Sohal, V.S., Deisseroth, K., Hegemann, P., 2010. Ultrafast optogenetic control. *Nat Neurosci*.; 13(3):387–392.

Hales, C.M., Rolston, J.D., Potter, S.M., 2010. How to culture, record and stimulate neuronal networks on micro electrode arrays (MEAs) J Vis Exp.; 30(39):2056.

Kale, R., P., Kouzani, A., Z., Walder, K., Berk, M., Susannah J. Tye, S., J., 2015. Review: Evolution of optogenetic microdevices, Neurophotonics, vol 2(3), 031206.

Kim, T., I., McCall, J., G., Jung, Y., H., Huang, X., Siuda, E., R., Li, Y., Song, J., Song, Y., M., Pao, H., A., Kim, R., H., Lu, C., Lee, S., D., Song, S., Shin, G., C., Al-Hasani, R., Kim, S., Tan, M., P., Huang, Y., Omenetto, F., G., Rogers, J., A., Bruchas, M., R., 2013. Injectable, cellular-scale optoelectronics with applications for wireless optogenetics, *Science*, vol. 340, pp. 211–216.

Kozai, T., D., Y., Vazquez, A., L., 2015. Photoelectric artefact from optogenetics and imaging on microelectrodes and bioelectronics: new challenges and opportunities, J. Mater. Chem. B, vol. 3, pp.4965-4978.

Krook-Magnuson, E., Armstrong, C., Bui, A., Lew, S., Oijala, M., and Soltesz, I. 2015. In vivo evaluation of the dentate gate theory in epilepsy. *J. Physiol*.

Lin, J.,Y., Lin, M.Z., Steinbach, P., Tsien, R.,Y., 2009. Characterization of engineered channelrhodopsin variants with improved properties and kinetics. *Biophys* J 96: 1803–1814.

Losonczy, B.V. Zemelman, A. Vaziri, et al.: Network mechanisms of theta related neuronal activity in hippocampal CA1 pyramidal neurons, Nat. Neurosci., vol. 13, pp. 967–972, 2010.

Nagel, G., Szellas, T., Huhn, W., Kateriya, S., Adeishvili N, Berthold, P., Ollig, D., Hegemann, P., Bamberg, E., 2003. Channelrhodopsin-2, a directly light-gated cation-selective membrane channel. Proc Natl Acad Sci USA 100: 13940–13945.

Ozden, I., Wang, J., Lu, Y., May, T., Joonhee Lee, J., Goo, W., Shea, D.J., Kalanithi, P., Diester, I., Diagne, M., Deisseroth, K., Shenoy, K.V., Arto V. NurmikkO, A.V., 2013. A coaxial optrode as multifunction write-read probe for optogenetic studies in non-human primates. J. Neurosci. Meth. 219, 142– 154.

Packer, A.M., Russell, L.E., Dalgleish, H.W.P., and Hausser, M., 2015. Simultaneous all-optical manipulation and recording of neural circuit activity with cellular resolution in vivo. Nat. Methods 12, 140–146.

Pisanello, F., Sileo, L., Oldenburg, I., A.3, Pisanello, M., Martiradonna, L., Assad, J., A., Sabatini, B., L., De Vittorio, M., 2014. Multipoint-emitting optical fibers for spatially addressable in vivo optogenetics," Neuron 82(6), 1245–1254.

Rays A., G., Fibers C., S., M., 1991. *Fiber optics*.

Riahi, E., Arezoomandan, R., Fatahi, Z., Haghparast, A., 2015. The electrical activity of hippocampal pyramidal neuron is subjected to descending control by the brain orexin/hypocretin system, Neurobiol. Learn Mem., 119, 93–101.

Royer, S., Zemelman, B., V., Barbic, M., Losonczy A, Buzsáki, G., Magee, J., C., 2010. Multi-array silicon probes with integrated optical fibers: Light-assisted perturbation and recording of local neural circuits in the behaving animal, Eur. J. Neurosci., vol. 31, pp. 2279–2291.

Sileo, L., Pisanello, M., Patria, A., D., Emhara, M., S., Pisanello, F., Massimo De Vittorio,M., 2015. Optical Fiber Technologies for in-vivo Light Delivery and Optogenetics. *Transparent Optical Networks (ICTON)*.

Sparta, D., R., Stamatakis, A., M., Phillips, J., L., Hovelsø, N., Van Zessen, R., Stuber, G., D., 2012. Construction of implantable optical fibers for long-term optogenetic manipulation of neural circuits, *Nature Protocols*, vol. 7, pp. 12-23.

Tufail, Y., Matyushov, A., Baldwin, N., Tauchmann, M.L., Georges, J., Yoshihiro, A., Tillery, S.I., Tyler, W.J., 2010. Transcranial pulsed ultrasound stimulates intact brain circuits. Neuron. 66(5):681–694.

Vo-Dinh, T., 2003. *Biomedical Photonics Handbook* (Boca Raton, FL: CRC Press).

Warden, M., R., Cardin, J., A., K. Deisseroth, K., 2014. Optical neural interfaces, *Annu. Rev. Biomed. Eng.*, vol. 16, pp. 103-129.

Wu, F., Stark, E., Im, M., Cho, I., J., Yoon, E., S., Buzsáki, G., Wise, K., D., Yoon, E., 2013. An implantable neural probe with monolithically integrated dielectric waveguide and recording electrodes for optogenetics applications, *Journal of Neural Engineering*, vol. 10, pp. 056012.

Yizhar, O., Fenno, L., E., Davidson, T., J., Mogri, M., Deisseroth, K., 2011. Optogenetics in neural systems, *Neuron*, vol. 71, pp. 9-34.

Zhang, F., Wang, F.L., Boyden, E.S., Deisseroth, K., 2006. Channelrhodopsin-2 and optical control of excitable cells, *Nat. Methods 3*(10), 785-792.

Zhang, F., V. Gradinaru, V., A.R. Adamantidis, A., R., , Durand, R., Airan, R., D., de Lecea, L., Deisseroth K., 2010. Optogenetic interrogation of neural circuits: Technology for probing mammalian brain structures, *Nat. Protocols*, vol. 5, pp. 439–456.

Zimmermann, D, Zhou, A., Kiesel, M., Feldbauer K., Terpitz, U., Haase, W., Schneider-Hohendorf, T., Bamberg, E., Sukhorukov, V.L., 2008. Effects on capacitance by overexpression of membrane proteins. Biochem Biophys Res Commun 369: 1022–1026.

Zorzos, A., N., Scholvin, J., Boyden, E., S., Fonstad, C., G., 2012. 3-dimensional multiwaveguide probe array for light delivery to distributed brain circuits, *Opt Lett.*, vol. 37, pp. 4841–4843.